Microwave gas sensor based on graphene aerogels

Yang Wu, *Member, IEEE*, Gabriele Restifo Pecorella, Gianluca Verderame, Daniele Annicchiarico, Thanuja Galhena, Stephen Hodge, Hannah Joyce, *Member, IEEE*, Patrizia Livreri, *Member, IEEE*, Antonio Lombardo, *Member, IEEE*

***Abstract*— In this article, the experimental demonstration of a novel microwave gas sensor based on graphene aerogel is presented. This device makes use of a highly porous structure of the aerogel in combination with the modulation of graphene AC conductivity upon exposure to vacuum and ambient air. As a proof of concept, we integrate the graphene aerogel into rectangular waveguides and measure its scattering parameters by a Vector network Analyzer (VNA). The aerogel is characterized by a combination of scanning electron microscopy and four-probe DC measurements. The aerogel is integrated into WR-90 waveguides by custom-designed support and wave propagation is tested over the 8-12 GHz frequency range (X-band). By exposing the aerogel to either air or a moderate vacuum, clear shifts in the waveguide scattering parameters are observed. In particular, changes of $\approx$ 3 dB and $\approx$ 1 dB in the transmission and reflection parameters of the waveguide are obtained, respectively. Moreover, the sensor exhibits excellent reproducibility when exposed to alternating cycles of air and vacuum, proving that the shifts in microwave transmission and reflection are caused by changes in the conductivity of the graphene aerogel due to the absorption and desorption of gas molecules. These proof-of-concept results pave the way for the development of a new class of gas sensors for applications such as breath analysis.**

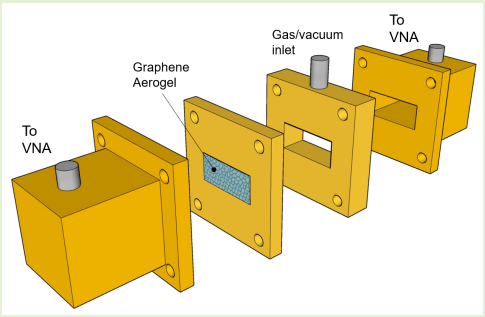

***Index Terms*— Gas sensor, graphene, graphene aerogel, microwave.**

I. Introduction

GAS sensors are widely used in numerous applications including chemical process control, medical diagnostics, industrial manufacturing safety, laboratories, agriculture, and environmental monitoring. They detect the presence and monitor the concentration of various gas species or volatile organic compounds (VOCs) and are used in particular to identify those that are pollutant, toxic, explosive, or hazardous, such as CO_2, NO_x, CO, CH_4, SO_x, HCHO, etc. Gas sensors are also used to monitor relative humidity (RH), for example in automotive applications [1]–[3]. Gas sensors are normally classified according to their working principles and sensing materials, and the most commonly used are: solid state (semiconductor, catalytic combustion, solid electrolyte, etc.) [4], aqueous electrochemical, paramagnetic, photometric (optical), thermal conductivity and acoustic [5]–[9].

An alternative approach to gas sensing is provided by microwave sensors. Microwaves interact differently with different materials according to their dielectric properties, causing frequency-dependent reorientation of molecular dipoles and motion of mobile charges [10]. Microwave sensors harness such effects, by enabling the interaction of an electromagnetic wave with the substance to be tested [11]. The frequency-dependent molecular polarization can be described by a complex permittivity as $\epsilon = \epsilon' + j\epsilon''$ [12]. The capacitive effect of the molecules in the substance is related to the real part of the complex permittivity of the sensing material, while the conductivity of the substance is related to the imaginary part [13]. The analyte modifies the wave propagation by causing magnitude attenuation and phase delay to the incident wave [13], and the analysis of the frequency-dependent transmission and reflection parameters enables the identification of the "dielectric signature" of the analyte and therefore its identification. Further in-depth theoretical explanation can be found in [14]. Microwave sensors can either be narrowband (resonators) or broadband (waveguides) and typically consist of metallic structures, such as coplanar or microstrip waveguides, where the fringing field is responsible for the interaction with an

Manuscript received 25 March 2023; accepted 5 July 2023. (Corresponding author: Antonio Lombardo)

Yang Wu and Hannah J. Joyce are with the Department of Engineering, University of Cambridge, Cambridge, CB3 0FA, U.K. (email: yw512@cam.ac.uk and hannah.joyce@eng.cam.ac.uk).

Gabriele Restifo Pecorella and Gianluca Verderame are with the Department of Engineering, University of Palermo, 90128, Palermo, Italy (email: gabriele.restifopecorella@community.unipa.it and gianluca.verderame@community.unipa.it)

Daniele Annicchiarico, Thanuja Galhena, and Stephen Hodge are with Versarien plc.

Patrizia Livreri is with the Department of Engineering, University of Palermo, 90128, Palermo, Italy, and with San Diego State University SDSU, CA, USA (email: patrizia.livreri@unipa.it)

Antonio Lombardo is with the London Centre for Nanotechnology & Department of Electronic and Electrical Engineering, University College London, London, WC1H 0AH, U.K.(email: a.lombardo@ucl.ac.uk).

analyte deposited on top of the waveguide. In metallic sensors, the sensing is entirely due to changes in analyte permittivity, which results in poor sensitivity, especially for broadband gas sensors [11]. A solution to this problem can be offered by graphene, a two-dimensional sheet of sp^2-hybridized carbon, whose microwave conductivity is high enough to support wave propagation and -at the same time- strongly modulated by adsorption of gas species on its surfaces. Moreover, graphene's AC conductivity is frequency-independent up to hundreds of GHz, its surface can be chemically functionalized to selectively bind with specific species and its atomic-thickness results in extremely high surface to volume ratio, thus offering an ideal platform to combine microwave broadband sensing and chemical field-effect sensing and achieve extremely high sensitivity [15]–[17].

Significant effort has been devoted into the relatively new field of microwave gas sensing. Different microwave structures, including resonator, split-ring resonator, double split-ring and microstrip resonators, coplanar waveguide, interdigital capacitor, coaxial structure, hybrid coupler, patch antennas, have been used to detect various gases and vapors such as acetone, ethanol, ammonia, nitrogen, benzene, methanol, toluene, water, etc [12], [18]. In 2013, Rossignol et al. detected 0-2000 ppm toluene and 0-500 ppm ammonia with a CoPc-covered (cobalt phthalocyanine) coplanar waveguide at room temperature [13]. In 2016, Bailly et al. achieved microwave ammonia (100-500 ppm) gas sensing at room temperature using coplanar waveguides [19] and a microstrip interdigital capacitors [18]. In 2020, Mohammadi et al. reported a differential gas sensor with two independent split-ring resonators in a power splitter/combiner configuration, able to detect the concentration of acetone vapor in both high and low concentrations with respective sensitivities of 0.01-0.02 mdB/ppm [20]. In 2022, Wang et al. selectively detected ammonia with a SnO_2/BP carbon based resonator at 2.56 GHz, with a limit of detection of 10 ppm [21]. Zhang et al. utilized variation of energy loss as sensor response signal for microwave gas sensor. Using this signal analysis method, they were able to achieve, on a narrow band-stop filter with graphite powder coating, a low detection limit of 1 ppm ammonia at room temperature, as well as good selectivity, 20-95$\%$ relative-humidity (RH) humidity-resistance, and good linearity in both low (1-5 ppm) and high (10-200 ppm) concentration ranges [22]. McClelland et al. reported an RH detection method by terminating an open-ended microwave waveguide resonator with piece of film of an organic electronic material, namely poly (3,4 ethylenedioxythiophene):poly(styrene sulfonate), or PEDOT:PSS. With the variation in resonant frequency and amplitude, RH values in the range of 0$\%$ to 85$\%$ could be detected [23]. In 2023, Maryam Moradpour et al. incorporated PEDOT:PSS to their rectangular split-ring resonator (SRR) for ammonia sensing. This organic microwave resonator (OMR) exhibited a sensitivity of 9.4 mdB/ppm, good repeatability of less than 5$\%$ variation, limit of detection of 1.3 ppm for ammonia, while barely responding to the interferant gases, proving good selectivity [24]. Wang et al., using a PANI-SnO_2 (polyaniline) based ultra-narrowband microwave filter transducer, selectively detected low concentration ammonia (7 ppm) with high sensitivity (S = 0.003 dB/ppm), fast response speed (response time τ_{res} = 40 s), and anti-humidity capacity (20 $\%$- 70 $\%$ RH) [25]. Most of the materials used as sensitive material are mainly metal oxide or conductive polymers.

Motivated by the need of increasing the surface area of graphene microwave gas sensors while keeping a small form-factor, we designed and computationally investigated a novel microwave sensor using three-dimensional macroassemblies of graphene sheets, known as graphene aerogels (GAs), which we integrated within a rectangular waveguide coupled with a gas inlet [26]. In GAs, graphene sheets form an interconnected network [27], leading to a highly porous structure ideal for gas sensing. Typically, a macroscopic 3D graphene structure would have at least one dimension exceeding 100 μm, with density below 0.1 $\mathrm{g/cm^3}$ and surface area ranging from 500 to 1000 m^2/g [28]. GAs are produced via hydrothermal reduction, chemical reduction, cross-linking, or template-directed method. GAs are characterized by high porosity and high surface area, as well as high electrochemical and cyclic stability [29], [30]. GAs have been used for energy storage in lithium ion batteries [31], environmental protection such as oil absorption [32], as well as electromagnetic interference (EMI) shielding. GA have also been used for DC gas sensors by functionalizing its surface with nanoparticles like SnO_2 [33], ZnO [34], and Pt [35], or with two dimensional transition metal dichalcogenides (TMDs) like WS_2 [36] and MoS_2 [37]. For example, for nanoparticles, in 2014, Anna Harley-Trochimczyk et al. fabricated low power hydrogen sensors by loading graphene aerogel with polysilicon microheaters functionalized by platinum nanoparticle catalyst. At the baseline temperature of 320 $^\circ$C, the sensors presented a sensitivity of 1.36$\%$/10000 ppm hydrogen, response and recovery times of 0.97 s and 0.72 s, a lower detection limit of around 65 ppm, and good selectivity against methane, n-pentane, and diethyl ether [35]. In the same year, Xin Liu et al. fabricated three-dimensional (3D) graphene aerogel-supported SnO_2 (SGA) nanoparticles. Using this SGA, they were able to detect NO_2 of concentrations ranging from 10 to 200 ppm in real time at room temperature with good linearity, sharp response, and good reversibility. For 50 ppm NO_2, the response was around 6$\%$ with response/recovery times of 190 s and 224 s. It also exhibited a superior selectivity against CO, H_2, NH_3, etc. Graphene aerogel was an indispensable part in the composite, where its large specific surface area allowed more surface active sites and highly effective surface interactions. It enhanced the sensitivity, exceeding that of the 2D graphene-SnO_2 counterpart, with not only the conductive network of the graphene sheets, but also the p-n junctions they formed at the interfaces with SnO_2. Its high porosity also provided gas transport pathways to accelerate the gas diffusion, adsorption, and desorption, facilitating fast response at low (room) temperature [33]. Then in 2015, based on the same ideology, they prepared a graphene-aerogel-ZnO sphere composite, where graphene aerogel acted as confined support to maintain the size and dispersion of the ZnO spheres aside from the benefits mentioned above. Again, they achieved room temperature detection of 10-200 ppm NO_2. For 50 ppm NO_2, the response was around 8$\%$, with response and recovery times

of about 132 s and 164 s [34]. In 2016, Hu Long et al. synthesized a MoS_2/graphene hybrid aerogel for NO_2 sensing [37]. In 2018, Wenjun Yan et al. investigated the performance tuning of NO_2 gas sensor based on WS_2/graphene aerogel composite by of ambient humidity and temperature [36]. In both scenarios, graphene aerogel were providing high specific surface area and high electrical and thermal conductivity. Non-functionalized graphene-foam has been used to achieve proof-of-concept NH_3 and NO_2 room temperature and atmospheric via monitoring the change in DC resistance [38]. best of our knowledge, the use of graphene aerogel for microwave gas sensing application has not been experimentally demonstrated. In our previous work, we developed a model to simulate GAs at microwave frequencies and showed that, when incorporated in a waveguide, variations of GA's chemical potential due to absorption of gas molecules alter both transmission and reflection parameters of the waveguide, significantly enhancing the variation due to direct interaction of the propagating wave with the gases [26].

In this article, we experimentally demonstrate that the GA microwave conductivity varies upon exposure to air or vacuum, and that, therefore, sensors can be made by using this highly-porous material, as predicted by our simulations [26]. The article is organized as follows. Section II introduces the transport properties of graphene at RF and microwave frequencies. In Section III, the sensor design is presented. A details aerogel preparation and integration into rectangular waveguides is reported in Section IV.A; Section IV.B summarizes the aerogel morphological and electrical characterization. Section IV.C discusses the microwave response of the sensor when exposed to air or vacuum. Section IV provides the conclusions.

II. Graphene transport properties at RF and Microwaves

The conductivity σ of single layer graphene from DC to optical frequencies is described by the Kubo formula [39]. This formalism takes into account both inter- and intra-band contributions. However, considering moderate values of chemical potential μ_c, the energy of the electromagnetic waves from DC to THz frequencies is insufficient for interband transition. When $\hbar\omega < 2|\mu_c|$ [40]–[42], it is therefore possible to neglect the inter-band transitions and express the dynamic conductivity of graphene only by the intra-band term of the Kubo formula as [41]:

$$\sigma_{\text{intra}}\left(\omega, E_F, \tau, T\right) = i\frac{\mathrm{e}^2 k_B T}{\pi\hbar^2\left(\omega - i\tau^{-1}\right)}\left[\frac{E_F}{k_B T} + 2\ln\left(1+\mathrm{e}^{-\frac{E_F}{k_B T}}\right)\right] \tag{1}$$

where:
$\omega = 2\pi f$ is the angular frequency,
E_F is the Fermi energy (also called chemical potential μ_c),
τ is the scattering time assumed to be independent of energy,
T is the temperature expressed in Kelvin,
$e \approx 1.6 \cdot 10^{-19}$ C is the electron charge,
$\hbar = \frac{h}{2\pi}$ is the reduced Planck's constant,
$k_B \approx 1.38 \cdot 10^{-23}\ \frac{\text{J}}{\text{K}}$ is the Boltzmann's constant,

Equation (1) shows how changes in Fermi level (chemical potential) induced by molecules or compounds adsorbed on the graphene surface modify its DC and AC conductivity, leading to modification of wave propagation [26]. The modification of graphene conductivity by gas adsorbates takes place via a direct charge transfer mechanism, where graphene Fermi level is shifted depending on its relative position with respect to the HOMO/LUMO of the adsorbed gas molecules [43], [44]. Gases such as CO, NH_3 and NO act as electron donor, resulting in n-doping of graphene, whereas gases such as O_2, H_2O and CO_2 act as electron acceptor, leading to p-doping [44].

III. Graphene aerogel-based microwave gas sensor design

In Fig. 1, the schematic model of the designed graphene aerogel-based microwave gas sensor is shown. The sensor is based on graphene-aerogel (GA) not chemically modified or functionalized and integrated, as a proof of concept, between two coaxial-to-rectangular waveguide (WR-90) adapters. A specially sample holder, shown at the top right of Fig. 1, was designed to support the graphene-aerogel and enable its integration in wave path. The sample holder has an opening whose area is equal to the section of the WR-90 (22.86 x 10.16 mm^2) and its thickness is equal to that of the GA sample (0.5 mm). The holder containing the GA sample is positioned in the middle of the structure to interact with the propagation of electromagnetic waves. An additional custom-made waveguide extension is included in the assembly to enable gas inlet and outlet. The WR-90 has an area equal to 22.86 x 10.16 mm^2 and shows a fundamental mode cut-off frequency (f_{TE10}) at 6.557 GHz. So, in order to work only with the fundamental mode, the operating frequency range from 8 to 12 GHz (X-band) was considered. The overall length of the assembly (i.e. adapters, sample holder and gas inlet) is ≈ 10 cm.

IV. Experiments and Results

A. Aerogel preparation

The graphene aerogel is prepared via freeze drying of commercially available water-based graphene inks (Graphink 1021, Versarien Plc). The inks are cast into custom-made "moulds" consisting of stainless steel frames of size $41\,\text{mm} \times 41\,\text{mm}$ and thicknesses $\approx 500\,\mu\text{m}$ mounted onto stainless steel blocks of size $41\,\text{mm} \times 41\,\text{mm} \times 5\,\text{mm}$. The blocks close one of the two sides of the frames, creating a well capable of holding the ink for the freeze drying process. The frames have a rectangular opening of $23\,\text{mm} \times 10\,\text{mm}$ at their centre, matching with the inner dimension of rectangular waveguides working in the X band. A layer of Kapton tape is placed between the frame and the base block in order to provide mechanical support to the aerogel during removal of the base. Once the well is filled with graphene ink, a quick quenching is performed by immersing the filled mould in liquid nitrogen: this step will freeze the water present in the ink which will

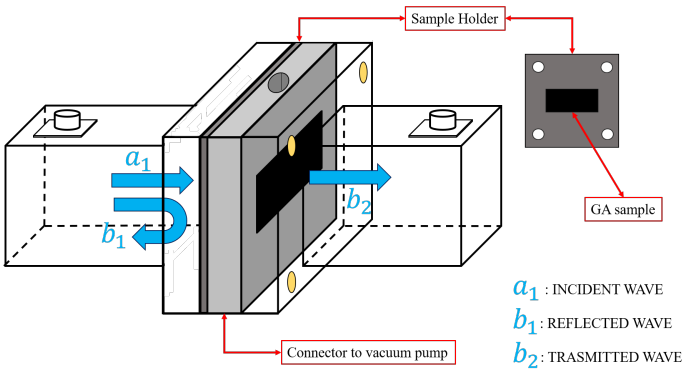

Fig. 1: Schematic view of the designed sensor composed of two coaxial-to-rectangular waveguide WR-90 adapters coupled to the GA by a custom-made holder. An additional custom-made waveguide extension is included in the assembly to enable connection to a vacuum pump and expose the GA to cycles of vacuum and air.

turn into ice. The samples are then transferred into a Telstar LyoQuest freeze dryer and kept under vacuum for 12 hrs, with a final pressure of 0.03-0.02 mbar. At the end of the cycle, the vacuum pump is switched off and the air carefully reintroduced into the chamber. Illustration of aerogel production process is presented in Fig. 2. Fig 2(a) shows the moulds filled with ink, while (b) shows the rapid cooling achieved by pouring liquid nitrogen and (c) the samples during the drying process. Fig 2(d) shows a representative aerogel sample deposited into a mould.

B. Aerogel characterization

The morphology of the graphene aerogel is characterized by a scanning electron microscopy (SEM) using an FEI Magellan 400 system. Fig. 3 shows the microscopic structure of a representative aerogel sample, which consists of a highly porous structure (pore size $\approx$ 50 - 100 μm) and tightly packed graphene flakes as sidewalls. This structure ensures a large surface to volume ratio, which maximize the interaction with the gas and therefore the resulting changes in GA RF conductivity.

DC sheet resistance of five different GA samples is measured with Keithley 6 1/2 digit multimeter and Jandel 4 point probe head. The sheet resistance is calculated by multiplying the readout from multimeter by a geometrical correction factor of 4.532. The results are summarized in Table I. Each sample is represented by the average sheet resistance measured in three different locations across the sample. It can be seen in Table 1 that the individual average sheet resistance is relatively similar to the overall average of 198.23 ohms per square ($\Omega/\square$), or an overall average sheet conductance of 5.09 millisiemens-square (mS·$\square$), where the standard deviation (SD) and standard error of mean (SEoM) values are relatively large due to the limitation of the sheet resistance measurement where the probe tips are puncturing the non-uniform graphene aerogel and the current paths formed between the probe tips are relatively random, leading to the variations.

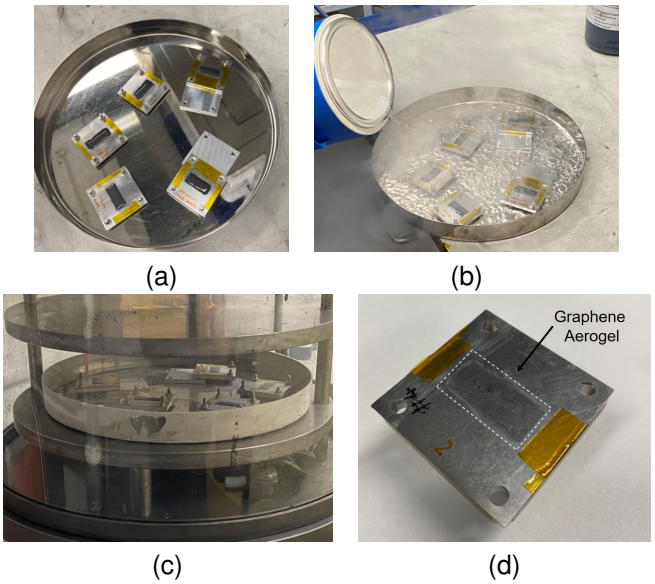

Fig. 2: Aerogel production process (a) Graphene ink is cast into metallic moulds. (b) Liquid nitrogen is poured onto the samples, resulting in rapid freezing of the water in the ink. (c) Samples mounted into the freeze drier system, where the water sublimates, resulting in a three-dimensional macroassemblies of graphene sheets. (d) Finished GA sample deposited into a frame and ready to be inserted into the rectangular waveguide assembly.

TABLE I: Sheet Resistance

	Sheet Resistance ($\Omega/\square$)				Sheet Conductance (mS·$\square$)	Uncertainty of sheet resistance	
Sample ID	1^{st}	2^{nd}	3^{rd}	Average	Average	SD	SEoM
A	351.43	206.21	178.67	254.44	3.93	43.76	25.26
B	202.18	212.93	170.71	195.27	5.12	10.34	5.97
C	170.61	215.73	191.57	192.64	5.19	10.64	6.14
D	220.08	184.44	159.55	188.02	5.32	14.34	8.28
E	153.90	221.37	134.09	169.79	5.89	21.57	12.45
Overall average sheet resistance	198.23	Overall average sheet conductance	5.09	Overall SD	48.1982	Overall SEoM	12.44

C. Gas sensing

GAs are inserted in the wave path of a rectangular waveguide, as schematically illustrated in Fig. 4. The frame containing the GA is sandwiched between two Advanced Technology Materials Inc. rectangular to coaxial adapters, which are in turn connected to an Agilent Technologies PNA-X vector network analyzer (VNA). A custom-designed additional rectangular waveguide element is added in the assembly to enable gas inlet/outlet. For this proof-of-concept implementation, the assembly is connected to a house vacuum line, enabling alternative exposure of the GA to air or vacuum. Parafilm was wrapped around the edges of the waveguide connection to provide better sealing. The gas inlet/outlet element is connected to the slide containing the GA ensuring to expose the part of the GA not supported by Kapton. The measurement setup, including a close-view of of the assembly is shown in Fig. 4.

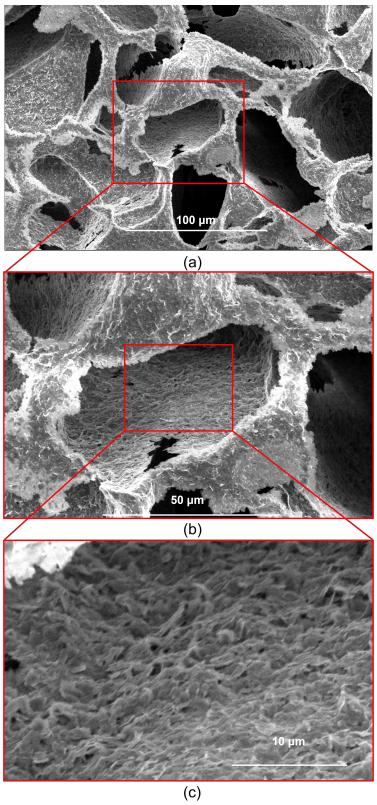

Fig. 3: SEM images of the same spot on one piece of GA fragment taken from sample with descending scales. (a) 100 um (b) 50 um (c) 10 um

At first, the VNA was calibrated using an Agilent Technologies N4693A E-calibration kit to move the reference plane to the end of the connections to the waveguide adapters as well as providing an evaluation for the level of systematic error [45]. Then, before measuring GA samples scattering parameters, baselines were established for the waveguide components. First, the waveguide assembly (i.e. coaxial to rectangular adapters, an empty frame and the gas inlet/outlet element) was measured under air and vacuum condition. Fig. 5 shows the S_{21} parameter for the two cases, showing no appreciable differences. In order to consider any possible effect resulting from the Kapton tape used as mechanical support for the GA, the same assembly is measured while covering a side of the (empty) frame by Kapton in air and vacuum. The results are plotted in Fig. 5, showing that Kapton tape is causing less than 0.2 dB reduction in the S_{21} parameter and negligible differences between air and vacuum. Fig. 5 also provides an estimation of the systematic error introduced by using an E-calibration kit at the cable termination instead of the more commonly used mechanical calibration kit at the waveguide adapters [45]. The black curve (which is equivalent to a thru device), shows a max S_{21} variation of ≈ 0.075 dB_{PP}, slightly larger than the commonly accepted value 0.017 dB_{PP} dB for a mechanical thru [45]. However, this error is very small compared to the S_{21} parameters of the sensors reported below. Moreover, we note that, for the particular VNA and calibration kit used, a magnitude uncertainly of ≈ 0.2 dB is expected for transmission coefficients in the range 0 to -20 dB and frequencies between 2 and 26.5 GHz [46]. Therefore, the systematic error introduced by the calibration method chosen is negligible.

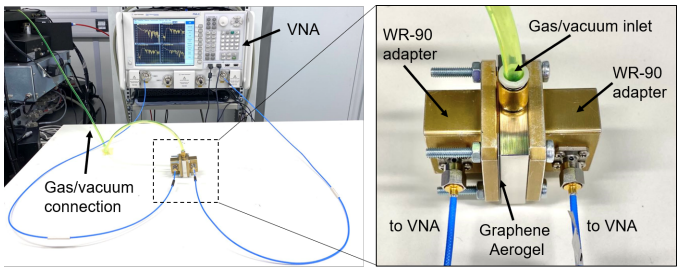

Fig. 4: Measurements setup, consisting of VNA, coaxial cables, gas pipe, coaxial to rectangular adaptors, aerogel holder, and gas inlet. (c) A close-up of the waveguide adaptors, aerogel holder, and gas inlet.

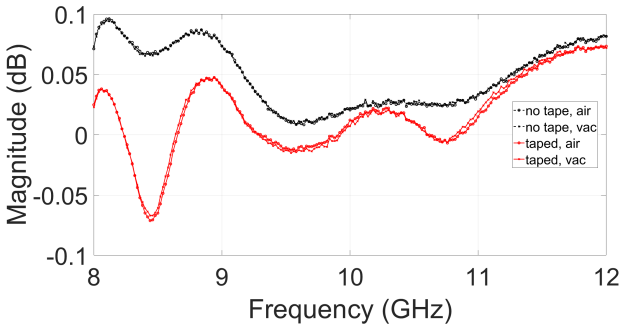

Fig. 5: S_{21} parameter of the waveguide assembly without aerogel when exposed to air or vacuum. The black curves correspond to the empty assembly, whereas in the red curves a layer of Kapton tape (identical to the one used to mechanically support the aerogel) has been introduced in the path of the propagating wave.

GAs are introduced into the waveguide using the frames discussed above. Transmission and reflection parameters are measured over the 8-12 GHz frequency range. The aerogel is exposed to cycles of ambient air (with relative humidity of $\approx$37.5% and temperature $\approx$20.2 $\pm$ 0.2 °C) and vacuum (with pressure of $\approx$91 mbar) and scattering parameters are acquired after 1 minute of stabilization. The results of the first two cycles are shown in Fig. 6. The transmission (S_{21}) and reflection (S_{11}) parameters of the waveguide are measured at each cycles, revealing a clear increase of transmission and reduction of reflection upon removal of air. The response is $\approx$ 3 dB for S_{21} and $\approx$ 1 dB in S_{11}. This is in clear contrast with the case of the "empty" waveguide shown in Fig. 5 where there is only negligible difference between air and vacuum, confirming GAs can be used as microwave gas sensor. The increase in transmission and reduction of reflection under vacuum can be interpreted as results of reduction of chemical doping in the GA due to the removal of air, which causes a decrease of the GA conductivity, facilitating wave transmission in the waveguide. This is consistent with previous studies

of graphene-based DC gas sensors and density functional theory (DFT) studies [43], [44], which showed that oxygen, carbon dioxide and moisture present in the air act as electron acceptors, thus p-doping the graphene (i.e. shifting the Fermi energy E_F to the valence band) and increasing its conductivity [43], [44]. In our experiment, by exposing the graphene to either ambient air with a relative humidity of ≈37.5% and temperature ≈20.2 ± 0.2 °C or to a moderate vacuum with pressure of ≈91 mbar, we cause absorption and desorption of gas molecules, respectively increasing and decreasing the (DC and AC) conductivity of the aerogel. The used setup, shown in Fig. 4, does not include mass-flow controllers, pressure gauges, humidity sensors, etc., and therefore it is not possible to estimate the sensitivity and compare it with other technologies used for microwave sensing, such as PEDOT:PSS [23], [24] or PDMS [20]. However, the scope of the present work is to provide an experimental proof-of-concept proving that graphene aerogel microwave conductivity is altered by exposure to gases and that, if incorporated in a waveguide, transmission and reflection parameters are modified much more significantly compared to metallic waveguides. For this reason and the limited sample size, an uncertainty analysis of RF measurements is not carried out, as for example in Ref. [47].

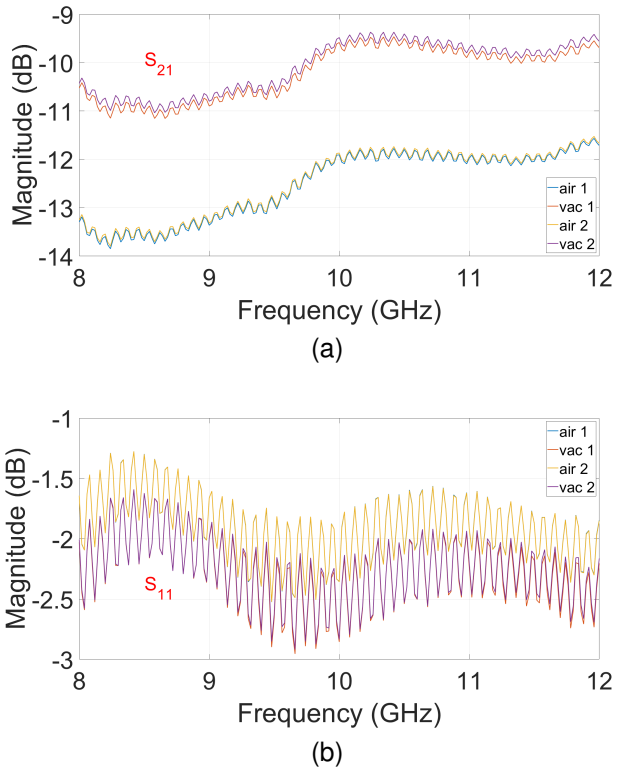

Fig. 6: Transmission (a) and reflection (b) parameters of the GA-based sensor exposed to air and vacuum across two cycles. The blue and yellow curves represent the S-parameters when the sensor is exposed to air while the purple and red curves correspond to vacuum.

Fig. 6 also evidences a very good reproducibility upon alternating exposure to air and vacuum. This is further confirmed by more extensive cycling between air and vacuum. In Fig. 7, the S_{21} values at an arbitrary frequency point (10.3 GHz) are extracted and plotted for 10 consecutive cycles to better illustrate the sensing response and reproducibility of the samples. As can be seen in the figure, a consistent ∼3 dB increase is obtained, with excellent reproducibility across the cycles and no need of any external intervention or re-setting.

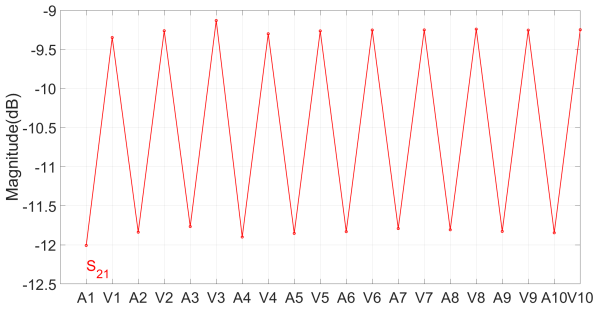

Fig. 7: S_{21} parameter at 10.3 GHz across 10 air-vacuum (A-V) cycles. A1 denotes the first exposure to air, A2 the second, and so on. Similarly, V1 indicates the first exposure to vacuum, V2 the second, etc.

V. Conclusions

This article provided the experimental implementation and characterization of a novel graphene aerogel-based sensor operating at X-band. By using commercially available water-dispersed graphene inks, we produced graphene aerogels within custom-designed holders and embedded them within rectangular waveguides connected to a vector network analyser via suitable adaptors. Using a custom-made waveguide extension, we exposed the aerogel to alternating cycles of ambient air (with relative humidity of ≈37.5% and temperature ≈20.2 ± 0.2 °C) and vacuum (with pressure of ≈91 mbar) and observed shifts ≈ 3 dB and ≈ 1 dB in the transmission and reflection parameters of the waveguide over the entire frequency range considered (8-12 GHz), respectively. Moreover, by repeating multiple air-vacuum cycles, the sensor showed very high reproducibility. These proof-of-concept results pave the way for the development of a new class of gas sensors for applications such as breath analysis.

Acknowledgments

AL acknowledges T. Hamer and J. Langdon for assistance with fabrication of the custom-made parts used in this work. YW acknowledges A. Curtis for assistance with the custom-made gas inlet and connection to vacuum and gas systems.

References

[1] N. Yamazoe, “Toward innovations of gas sensor technology,” *Sensors and Actuators B: Chemical*, vol. 108, no. 1, pp. 2–14, 2005. [Online]. Available: https://www.sciencedirect.com/science/article/pii/S0925400505000286

[2] J. Dai, O. Ogbeide, N. Macadam, Q. Sun, W. Yu, Y. Li, B.-L. Su, T. Hasan, X. Huang, and W. Huang, “Printed gas sensors,” *Chem. Soc. Rev.*, vol. 49, no. 6, pp. 1756–1789, 2020, publisher: The Royal Society of Chemistry. [Online]. Available: https://pubs.rsc.org/en/content/articlelanding/2020/cs/c9cs00459a

[3] S. Hong, M. Wu, Y. Hong, Y. Jeong, G. Jung, W. Shin, J. Park, D. Kim, D. Jang, and J.-H. Lee, "FET-type gas sensors: A review," *Sensors and Actuators B: Chemical*, vol. 330, p. 129240, 2021. [Online]. Available: https://www.sciencedirect.com/science/article/pii/S092540052031580X

[4] A. M. Azad, S. A. Akbar, S. G. Mhaisalkar, L. D. Birkefeld, and K. S. Goto, "Solid-state gas sensors: A review," *J. Electrochem. Soc.*, vol. 139, no. 12, pp. 3690–3704, 1992. [Online]. Available: https://iopscience.iop.org/article/10.1149/1.2069145

[5] R. Kocache, "Gas sensors," *Sensor Review*, vol. 14, no. 1, pp. 8–12, 1994, publisher: MCB UP Ltd. [Online]. Available: https://doi.org/10.1108/EUM0000000004256

[6] S. Dhall, B. R. Mehta, A. K. Tyagi, and K. Sood, "A review on environmental gas sensors: Materials and technologies," *Sensors International*, vol. 2, p. 100116, 2021. [Online]. Available: https://www.sciencedirect.com/science/article/pii/S2666351121000371

[7] S. Karthikeyan and H. Pandya, "Gas sensors- a review," *J. Environ. Nanotechnol.*,, vol. 4, no. 4, pp. 01–14, 2015. [Online]. Available: http://www.nanoient.org/JENT/Volume4/Issue4/Gas-Sensors--A-Review/436#.V0kElDV9600

[8] S. Fanget, S. Hentz, P. Puget, J. Arcamone, M. Matheron, E. Colinet, P. Andreucci, L. Duraffourg, E. Myers, and M. L. Roukes, "Gas sensors based on gravimetric detection—a review," *Sensors and Actuators B: Chemical*, vol. 160, no. 1, pp. 804–821, 2011. [Online]. Available: https://www.sciencedirect.com/science/article/pii/S0925400511007891

[9] A. Bogner, C. Steiner, S. Walter, J. Kita, G. Hagen, and R. Moos, "Planar microstrip ring resonators for microwave-based gas sensing: Design aspects and initial transducers for humidity and ammonia sensing," *Sensors*, vol. 17, no. 10, p. 2422, 2017. [Online]. Available: https://www.mdpi.com/1424-8220/17/10/2422

[10] A. Kremer, F. Scönhals, *Broadband Dielectric Spectroscopy*. Springer, 2003, vol. 16, no. 4.

[11] G. Guarin, M. Hofmann, J. Nehring, R. Weigel, G. Fischer, and D. Kissinger, "Miniature microwave biosensors: Noninvasive applications," *IEEE Microwave Magazine*, vol. 16, no. 4, pp. 71–86, 2015.

[12] F. Li, Y. Zheng, C. Hua, and J. Jian, "Gas sensing by microwave transduction: Review of progress and challenges," vol. 6, 2019. [Online]. Available: https://www.frontiersin.org/articles/10.3389/fmats.2019.00101

[13] J. Rossignol, G. Barochi, B. De Fonseca, J. Brunet, M. Bouvet, A. Pauly, and L. Markey, "Microwave-based gas sensor with phthalocyanine film at room temperature," *Sensors and Actuators B: Chemical*, vol. 189, pp. 213–216, 2013.

[14] W. Wang, R. Pradhan, Y. S. Ho, Z. Zhao, Q. Sun, X. Liao, S. Wang, Z. Fang, and Y. Zheng, "Mrc-based double figure-of-eight coil sensor system with triple-mode operation capability for biomedical applications," *IEEE Sensors Journal*, vol. 21, no. 13, pp. 14 491–14 502, 2020.

[15] P. Gubeljak, L. Pedrazzetti, O. J. Burton, L. Magagnin, S. Hofmann, G. G. Malliaras, and A. Lombardo, "Multi-dimensional microwave sensing using graphene waveguides," *2022 Ieee International Symposium on Medical Measurements and Applications (Memea 2022)*, 2022. [Online]. Available: ⟨GotoISI⟩://WOS:000861225100122

[16] P. Gubeljak, T. Xu, L. Pedrazzetti, O. J. Burton, L. Magagnin, S. Hofmann, G. G. Malliaras, and A. Lombardo, "Electrochemically-gated graphene broadband microwave waveguides for ultrasensitive biosensing," *arXiv:2210.14118*, 2022.

[17] C. J. Docherty, C.-T. Lin, H. J. Joyce, R. J. Nicholas, L. M. Herz, L.-J. Li, and M. B. Johnston, "Extreme sensitivity of graphene photoconductivity to environmental gases," *Nature Communications*, vol. 3, no. 1, p. 1228, Nov 2012.

[18] G. Bailly, A. Harrabi, J. Rossignol, D. Stuerga, and P. Pribetich, "Microwave gas sensing with a microstrip interdigital capacitor: Detection of nh3 with tio2 nanoparticles," *Sensors and Actuators B: Chemical*, vol. 236, pp. 554–564, 2016.

[19] G. Bailly, J. Rossignol, B. de Fonseca, P. Pribetich, and D. Stuerga, "Microwave gas sensing with hematite: Shape effect on ammonia detection using pseudocubic, rhombohedral, and spindlelike particles," *ACS Sensors*, vol. 1, no. 6, pp. 656–662, 2016.

[20] S. Mohammadi and M. H. Zarifi, "Differential microwave resonator sensor for real-time monitoring of volatile organic compounds," *IEEE Sensors Journal*, vol. 21, no. 5, pp. 6105–6114, 2020.

[21] N. Wang, N. Zhang, T. Wang, F. Liu, X. Wang, X. Yan, C. Wang, X. Liu, P. Sun, and G. Lu, "Microwave gas sensor for detection of ammonia at room-temperature," *Sensors and Actuators B: Chemical*, vol. 350, p. 130854, 2022.

[22] N. Zhang, B. Jiang, S. Xue, X. Wang, T. Wang, P. Sun, and G. Lu, "General analysis method for the signal enhancement of microwave gas sensor though variation of energy loss," *Sensors and Actuators B: Chemical*, vol. 367, p. 132117, 2022.

[23] J. McClelland, O. Niksan, and M. H. Zarifi, "Investigating a microwave waveguide sensor with an organic pedot: Pss boundary for humidity detection," in *2022 International Conference on Electrical, Computer and Energy Technologies (ICECET)*. IEEE, 2022, pp. 1–5.

[24] M. Moradpour, M. C. Jain, N. R. Tanguy, K. Colegrave, and M. H. Zarifi, "Exploring pedot: Pss interaction with hazardous gas molecules in microwave regime using organic microwave resonators," *Chemical Engineering Journal*, p. 141500, 2023.

[25] N. Wang, W. Tao, N. Zhang, T. Wang, X. Wang, F. Liu, X. Yan, F. Liu, X. Liang, P. Sun *et al.*, "Unlocking the potential of organic-inorganic hybrids in microwave gas sensors: Rapid and selective nh3 sensing at room-temperature," *Sensors and Actuators B: Chemical*, vol. 378, p. 133112, 2023.

[26] G. R. Pecorella, G. Verderame, P. Livreri, and A. Lombardo, "Microwave gas sensor based on graphene aerogel for breath analysis," in *2022 IEEE International Symposium on Medical Measurements and Applications (MeMeA)*, 2022, pp. 1–6.

[27] M. A. Worsley, P. J. Pauzauskie, T. Y. Olson, J. Biener, J. H. Satcher Jr, and T. F. Baumann, "Synthesis of graphene aerogel with high electrical conductivity," *Journal of the American Chemical Society*, vol. 132, no. 40, pp. 14 067–14 069, 2010.

[28] Z. Sun, S. Fang, and Y. H. Hu, "3d graphene materials: From understanding to design and synthesis control," *Chem. Rev.*, vol. 120, no. 18, pp. 10 336–10 453, 2020, publisher: American Chemical Society. [Online]. Available: https://doi.org/10.1021/acs.chemrev.0c00083

[29] G. Gorgolis and C. Galiotis, "Graphene aerogels: a review," *2D Mater.*, vol. 4, no. 3, p. 032001, 2017, publisher: IOP Publishing. [Online]. Available: https://doi.org/10.1088/2053-1583/aa7883

[30] J. Feng, B.-L. Su, H. Xia, S. Zhao, C. Gao, L. Wang, O. Ogbeide, J. Feng, and T. Hasan, "Printed aerogels: chemistry, processing, and applications," *Chem. Soc. Rev.*, vol. 50, no. 6, pp. 3842–3888, 2021. [Online]. Available: http://xlink.rsc.org/?DOI=C9CS00757A

[31] C. Tan, J. Cao, A. M. Khattak, F. Cai, B. Jiang, G. Yang, and S. Hu, "High-performance tin oxide-nitrogen doped graphene aerogel hybrids as anode materials for lithium-ion batteries," *Journal of Power Sources*, vol. 270, pp. 28–33, 2014. [Online]. Available: https://www.sciencedirect.com/science/article/pii/S0378775314011033

[32] H.-Y. Mi, X. Jing, A. L. Politowicz, E. Chen, H.-X. Huang, and L.-S. Turng, "Highly compressible ultra-light anisotropic cellulose/graphene aerogel fabricated by bidirectional freeze drying for selective oil absorption," *Carbon*, vol. 132, pp. 199–209, 2018. [Online]. Available: https://www.sciencedirect.com/science/article/pii/S000862231830157X

[33] X. Liu, J. Cui, J. Sun, and X. Zhang, "3d graphene aerogel-supported SnO 2 nanoparticles for efficient detection of NO 2," *RSC Advances*, vol. 4, no. 43, pp. 22 601–22 605, 2014, publisher: Royal Society of Chemistry. [Online]. Available: https://pubs.rsc.org/en/content/articlelanding/2014/ra/c4ra02453b

[34] X. Liu, J. Sun, and X. Zhang, "Novel 3d graphene aerogel–ZnO composites as efficient detection for NO2 at room temperature," *Sensors and Actuators B: Chemical*, vol. 211, pp. 220–226, 2015. [Online]. Available: https://www.sciencedirect.com/science/article/pii/S0925400515001094

[35] A. Harley-Trochimczyk, J. Chang, Q. Zhou, J. Dong, T. Pham, M. A. Worsley, R. Maboudian, A. Zettl, and W. Mickelson, "Catalytic hydrogen sensing using microheated platinum nanoparticle-loaded graphene aerogel," *Sensors and Actuators B: Chemical*, vol. 206, pp. 399–406, 2015. [Online]. Available: https://www.sciencedirect.com/science/article/pii/S0925400514011265

[36] W. Yan, M. A. Worsley, T. Pham, A. Zettl, C. Carraro, and R. Maboudian, "Effects of ambient humidity and temperature on the NO2 sensing characteristics of WS2/graphene aerogel," *Applied Surface Science*, vol. 450, pp. 372–379, 2018. [Online]. Available: https://www.sciencedirect.com/science/article/pii/S0169433218311577

[37] H. Long, A. Harley-Trochimczyk, T. Pham, Z. Tang, T. Shi, A. Zettl, C. Carraro, M. A. Worsley, and R. Maboudian, "High surface area MoS2/graphene hybrid aerogel for ultrasensitive NO2 detection," *Advanced Functional Materials*, vol. 26, no. 28, pp. 5158–5165, 2016, _eprint: https://onlinelibrary.wiley.com/doi/pdf/10.1002/adfm.201601562. [Online]. Available: https://onlinelibrary.wiley.com/doi/abs/10.1002/adfm.201601562

[38] F. Yavari, Z. Chen, A. V. Thomas, W. Ren, H.-M. Cheng, and N. Koratkar, "High sensitivity gas detection using a macroscopic three-dimensional graphene foam network," *Sci Rep*, vol. 1, no. 1, p.

166, 2011, number: 1 Publisher: Nature Publishing Group. [Online]. Available: https://www.nature.com/articles/srep00166
[39] R. Kubo, "Statistical-mechanical theory of irreversible processes. i. general theory and simple applications to magnetic and conduction problems," *Journal of the Physical Society of Japan*, vol. 12, no. 6, pp. 570–586, 1957.
[40] S. A. Awan, A. Lombardo, A. Colli, G. Privitera, T. S. Kulmala, J. M. Kivioja, M. Koshino, and A. C. Ferrari, "Transport conductivity of graphene at RF and microwave frequencies," *2D Mater.*, vol. 3, no. 1, p. 015010, 2016, publisher: IOP Publishing. [Online]. Available: https://doi.org/10.1088/2053-1583/3/1/015010
[41] G. W. Hanson, "Dyadic green's functions and guided surface waves for a surface conductivity model of graphene," *Journal of Applied Physics*, vol. 103, no. 6, p. 064302, 2008. [Online]. Available: http://aip.scitation.org/doi/10.1063/1.2891452
[42] J. Zhang and W. Zhu, "Graphene-based microwave metasurfaces and radio-frequency devices," *Advanced Photonics Research*, vol. 2, no. 11, p. 2100142, 2021, _eprint: https://onlinelibrary.wiley.com/doi/pdf/10.1002/adpr.202100142. [Online]. Available: https://onlinelibrary.wiley.com/doi/abs/10.1002/adpr.202100142
[43] F. Schedin, A. K. Geim, S. V. Morozov, E. W. Hill, P. Blake, M. I. Katsnelson, and K. S. Novoselov, "Detection of individual gas molecules adsorbed on graphene," *Nature Materials*, vol. 6, no. 9, pp. 652–655, 2007. [Online]. Available: ⟨GotoISI⟩://WOS:000249236200017,https://core.ac.uk/download/16122035.pdf
[44] D. J. Buckley, N. C. G. Black, E. G. Castanon, C. Melios, M. Hardman, and O. Kazakova, "Frontiers of graphene and 2d material-based gas sensors for environmental monitoring," *2D Materials*, vol. 7, no. 3, 2020.
[45] "Keysight technologies 11644a x, p, and k waveguide calibration kits." [Online]. Available: https://www.keysight.com/us/en/assets/9018-01043/user-manuals/9018-01043.pdf
[46] "Keysight downloadable vector network analyzer uncertainty calculator." [Online]. Available: www.keysight.com
[47] Z. Zhao, A. Weerasinghe, Q. Sun, F. Fan, and K. Y. See, "Improved calibration technique for two-probe setup to enhance its in-circuit impedance measurement accuracy," *Measurement*, vol. 185, p. 110007, 2021.

Yang Wu received his Bachelor's degree in Opto-Electronics Information Science and Engineering at Sun Yat-sen University in 2019. He is currently a PhD student with the Department of Engineering, University of Cambridge.

Gabriele Restifo Pecorella received his Bachelor's degree in 2020 and Master's degree in Electronic Engineering with honours and mention in 2022 at the University of Palermo, Italy. Now, he is a designer of IGBT and power bipolar transistors at STMicroelectronics.

Gianluca Verderame received his Bachelor's degree in 2020 and his Master's Degree in Modern Electronics with honor and with mention in 2022 both at the University of Palermo. Now, he is an Application Engineer in STMicroelectronics in Catania, Italy.

Daniele Annicchiarico received his Master's degree in 2006 at the University of Milano-Bicocca Italy and PhD's degree in 2014 at the Cranfield University, UK. Now, he is a Senior Application Scientist at Versarien plc.

Thanuja Galhena is an Engineering Fellow at Churchill college, University of Cambridge. Previously, she was a Senior Scientist at Versarien plc, a Postdoctoral Research Associate and a Teaching Fellow at the University of Cambridge. She holds a BSc from the University of Colombo, Sri Lanka, an M.Phil. and at PhD from University of Cambridge.

Stephen Hodge is Chief Technology Officer of Versarien plc and has a PhD in Nanomaterial Chemistry from Imperial College London. He has held post-doctoral research associate positions at the University of Cambridge. He is responsible for overseeing the company's graphene and related materials research and development activities and is a member of academic and industry committees. He was awarded the Royal Society of Chemistry 2022 Rising Star in Industry Award.

Hannah Joyce is a professor at the Department of Engineering at the University of Cambridge. Her research specialises in the development of new nanomaterials for applications in optoelectronics and energy harvesting. Joyce received a Bachelor of Science and Bachelor of Engineering in 2005 from the University of Western Australia. She obtained a Ph.D. in physics from the Australian National University in 2010.

Patrizia Livreri (M'90) PhD, is a Professor at the Department of Engineering, University of Palermo, and a Visiting Professor at the San Diego State University. She received her PhD in ICT in 1992 from the University of Palermo, Italy. She is the author or co-author of scientific books and more than 200 scientific publications. Her current research interests include microwaves, antennas, and radars.

Antonio Lombardo is a Lecturer in Nanostructure and Devices at the London Centre for Nanotechnology and the Electronic and Electrical Engineering Department, University College London. He obtained a a PhD from the University of Cambridge, UK (2014). His research is focussed on design, fabrication, and testing of novel electronic devices based on graphene and 2D materials, for applications in high frequency (bio)sensing and energy-efficient electronics.